

1 *An N-acetylglucosamine transporter required for arbuscular mycorrhizal symbiosis in rice and*  
2 *maize.*

3  
4 Marina Nadal<sup>1,2</sup>ψ, Ruairidh Sawers<sup>2</sup>ϣ, Shamoan Naseem<sup>3</sup>, Barbara Bassin<sup>4</sup>, Corinna Kulicke<sup>1</sup>¶,  
5 Abigail Sharman<sup>1</sup>, Gynheung An<sup>5</sup>, Kyungsook An<sup>5</sup>, Kevin R. Ahern<sup>6</sup>, Amanda Romag<sup>6</sup>, Thomas  
6 P. Brutnell<sup>6</sup>&, Caroline Gutjahr<sup>2</sup>§, Niko Geldner<sup>2</sup>, Christophe Roux<sup>7</sup>, Enrico Martinoia<sup>4</sup>, James B.  
7 Konopka<sup>3</sup> & Uta Paszkowski<sup>1, 2\*</sup>ψ

8  
9 <sup>1</sup>Department of Plant Sciences, University of Cambridge, Cambridge, CB2 3EA, UK.

10 <sup>2</sup>Department of Plant Molecular Biology, University of Lausanne, 1015 Lausanne, Switzerland.

11 <sup>3</sup>Department of Molecular Genetics and Microbiology, Stony Brook University, Stony Brook, NY  
12 11794-5222, USA.

13 <sup>4</sup>Institute of Plant Biology, University of Zurich, 8008 Zurich, Switzerland.

14 <sup>5</sup>Crop Biotech Institute and Graduate School of Biotechnology, Kyung Hee University, Yongin  
15 17104, Korea

16 <sup>6</sup>Boyce Thompson Institute for Plant Research, Ithaca, New York 14853, USA.

17 <sup>7</sup>Université de Toulouse, UPS, UMR5546, Laboratoire de recherche en Sciences Végétales, BP  
18 42617, F-31326 Castanet-Tolosan CEDEX, France.

19  
20 Present addresses:

21 <sup>ψ</sup>Laboratorio Nacional de Genómica para la Biodiversidad, Centro de Investigación y de Estudios  
22 Avanzados, Campus Guanajuato, PO Box 629, Irapuato Guanajuato, Mexico 36821.

23 <sup>&</sup>Donald Danforth Plant Science Center, 975 North Warson Road St. Louis, Missouri 63132,  
24 USA.

25

26 §Faculty of Biology, Genetics, University of Munich, 82152 Martinsried, Germany.

27 ¶Sir William Dunn School of Pathology, University of Oxford, South Parks Road, Oxford OX1

28 3RE, UK.

29

30 ψ These authors contributed equally to this work.

31 \*to whom correspondence should be addressed: Uta Paszkowski, up220@cam.ac.uk

32

33

34 **Abstract**

35 Most terrestrial plants, including crops, engage in beneficial interactions with arbuscular  
36 mycorrhizal fungi. Vital to the association is mutual recognition involving the release of  
37 diffusible signals into the rhizosphere. Previously, we identified the maize *no perception 1*  
38 (*nope1*) mutant defective in early signaling. Here, we report cloning of *ZmNOPE1* on the  
39 basis of synteny with rice. *NOPE1* encodes a functional homolog of the *Candida albicans*  
40 N-acetylglucosamine (GlcNAc) transporter *NGT1*, and represents the first plasma  
41 membrane GlcNAc transporter identified from plants. In *C. albicans*, exposure to GlcNAc  
42 activates cell signaling and virulence. Similarly, in *Rhizophagus irregularis* treatment with  
43 rice wild type but not *nope1* root exudates induced transcriptome changes associated with  
44 signaling function, suggesting a requirement of NOPE1 function for presymbiotic fungal  
45 reprogramming. (122 words)

46

47

48

## 49 **Introduction**

50 Arbuscular Mycorrhizal (AM) symbiosis entails a mutually beneficial relationship between  
51 plants and fungi in which plant roots exchange photoassimilated compounds for fungus-delivered  
52 soil mineral nutrients. The resulting interaction profoundly influences plant, including crop  
53 performance. For the symbiosis to begin, plant roots and AM fungi (AMF) signal each other in the  
54 soil via secretion of diffusible compounds <sup>1</sup>. These include fungal chitin-based molecules  
55 (reviewed in <sup>2,3</sup>), which are detected by the Lysin Motif (LysM) containing receptor-like kinases  
56 (RLKs) at the plasma membrane of legumes and rice, respectively <sup>4,5</sup>. Central for the perception of  
57 AMF however are the  $\alpha/\beta$  hydrolase DWARF 14 LIKE (D14L) and the F-box protein DWARF 3  
58 (D3) <sup>6</sup>. Mutations in either *D14L* or *D3* renders rice incapable of sensing the AMF and leads to the  
59 complete loss of susceptibility to the fungus <sup>6</sup>. The recognition substrate is at present unknown but  
60 could either be an AMF-released or a plant-derived molecule.

61 Several plant-derived factors are known to stimulate morphological changes in AMF that are  
62 thought to promote fungal-host encounters <sup>1</sup>. This includes flavonoids that promote AMF hyphal  
63 tip elongation <sup>7</sup>, 2-hydroxy fatty acids (2-OH-FA) triggering hyphal branching <sup>8</sup>, and root-  
64 secreted strigolactones (SL) that induce profuse hyphal ramification <sup>9</sup>. Moreover, the SL induced  
65 morphological switch is preceded by a sharp change in fungal metabolism characterized by  
66 increased cellular respiration, mitochondria biogenesis, and mitotic activity <sup>10,11</sup>. Despite their pre-  
67 symbiotic effect on AMF growth behavior, plant SL or flavonoid biosynthetic mutants are still  
68 partially or fully colonized, respectively <sup>12,13</sup>, and the relevance of 2-OH-FAs for symbiosis  
69 establishment is unknown. Once the fungus has reached the plant's surface, cutin monomers  
70 induce hyphopodium differentiation, the anchoring structure that aids AMF entering the root  
71 epidermal cell layer <sup>14</sup>. However, as the fungal genome lacks genes for the *de novo* biosynthesis of  
72 certain fatty acids <sup>15</sup> cutin may have in addition a nutritional role.

73 To better understand the mechanisms that lead to symbiosis establishment, we analyzed the  
74 maize *no perception1* (*nope1*) mutant which lacks proper hyphopodium differentiation on the root  
75 surface, suggesting an impairment in signaling between the fungus and the plant during pre-  
76 symbiotic signal exchange <sup>16</sup>. Interestingly, we found that *NOPE1* encodes an N-  
77 acetylglucosamine (GlcNAc) transporter, so far not described in plants but homologous to the  
78 Ngt1 transporter described in fungi <sup>17</sup>. This is significant as GlcNAc has been shown to stimulate  
79 the fungal pathogen *C. albicans* to undergo morphological changes and increase expression of  
80 virulence genes that promote pathogenic interactions with the host <sup>18</sup>. Our analyses provide the  
81 first evidence that a previously unknown plant GlcNAc transporter plays a role in the initiation of  
82 root colonization by AMF.

83

## 84 **Results**

### 85 **Cloning of maize *NOPE1* using synteny with rice**

86 The maize *nope1* mutant is unable to establish AM symbioses <sup>16</sup>. Limited physical interaction of  
87 *nope1* with AMF suggested a failure in pre-symbiotic plant-fungal recognition that preceded  
88 fungal colonization of the root. Genetic mapping linked the *NOPE1* locus to the marker  
89 UMC1336, located at 86.4 Mb on chromosome 10. On the basis of our previous molecular  
90 characterization of AM symbiosis in rice, we searched for rice candidate genes showing a  
91 transcriptional response to AMF located in a region syntenic to maize *nope1* <sup>19</sup>. **We identified the**  
92 **AM symbiosis-induced rice gene *LOC\_Os04g01520*, which showed a >6 fold induction in**  
93 **colonized relative to control roots (*OsAMI56* <sup>19</sup>), and was located at 0.4 Mb on rice chromosome 4**  
94 **(Figure 1A, underlined). According to rice expression atlas data, *LOC\_Os04g01520* transcripts**  
95 **accumulate to low levels across different plant organs, including leaves, stem and embryo tissue,**  
96 **with the highest accumulation in anthers (<http://ricexpro.dna.affrc.go.jp/>).**

97 *LOC\_Os04g01520* encodes a single copy gene in the rice genome. Based on full cDNA analysis  
98 (<http://getentry.ddbj.nig.ac.jp/getentry/ddbj/AK101964?filetype=html>) and supporting ESTs, the  
99 gene model predicted two exons and one intron (Figure 1B), producing an ORF of 1404 bp. The  
100 5' and 3' RACE PCR analysis indicated a transcriptional start point at -70 bp and a 184 bp 3'UTR  
101 sequence. The gene product of *LOC\_Os04g01520* consists of 476 residues and has a predicted  
102 molecular weight of 50.34 kD.

103 To investigate the role *LOC\_Os04g01520* plays during AM symbiosis, we identified two lines  
104 *4A-01057* and *3A-02512* from the POSTECH mutant collection <sup>20</sup> with T-DNA insertions 158 bp  
105 downstream of ATG within the first exon, and 22 bp upstream of the 3' intron splice-junction,  
106 respectively (Figure 1B). RT-PCR based analysis of *LOC\_Os04g01520* mRNA levels in line *4A-*  
107 *01057* using primers either spanning the insertion site or a more 3' region failed to detect  
108 transcript (Figure 1C). In line *3A-02512* however, transcripts of *LOC\_Os04g01520* accumulated  
109 to wild type size and levels, suggesting that the T-DNA insertion had been removed together with  
110 the intron during splicing, and therefore this allele was no longer considered for our study.  
111 Genomic PCR amplification and sequencing of the amplicon from line *4A-01057* confirmed  
112 mutation at the predicted site and revealed the additional presence of ~800 bp of the backbone  
113 vector (pGA2517) on the T-DNA right-border side (Figure 1B).

114 Co-cultivation of plants segregating for the T-DNA insertion *4A-01057* with *R. irregularis*  
115 identified a significant reduction ( $p \leq 0.05$  for all structures tested) of fungal root colonization in  
116 homozygous mutant plants (Figure 2A). Comparing fungal colonization structures on wild type  
117 and mutant roots showed aberrant hyphopodia on the root surface of *4A-01057* that were absent  
118 from wild type roots (Figure 2B-C). Closer inspection of hyphopodia morphology on *4A-01057*  
119 revealed multiple unsuccessful penetration attempts (Figure 2D, arrowheads) and extensive hyphal  
120 septation, a sign of fungal stress (Figure 2C, arrows). Infrequently, the fungus succeeded in  
121 invading the root cortex and produced arbuscules that were of wild type morphology (Figure 2E-

122 F). Germination, overall vegetative and reproductive development, and seed production of 4A-  
123 01057 plants were equivalent to the wild type. To corroborate that the mutant phenotype of line  
124 4A-01057 was indeed linked to the insertion at *LOC\_Os04g01520*, we reintroduced a wild type  
125 copy of the gene under the native promoter into line 4A-01057 and found that wild-type levels of  
126 AM fungal colonization were restored in eleven independent transformants (Figure 2A, G;  
127 Supplemental Figure S1), confirming that the mutation in gene *LOC\_Os04g01520* caused the AM  
128 phenotype of line 4A-01057. The quantitative and qualitative phenotype of the rice insertion  
129 mutant was thus equivalent to the reported maize *nope1* mutant<sup>16</sup> and the 4A-01057 allele was  
130 accordingly designated *OsNOPE1*.

131 To investigate whether NOPE1 was required for susceptibility to diverse fungal species,  
132 known to effectively invade rice roots<sup>21,22</sup>, wild type and *Osnope1* mutant roots were inoculated  
133 with *Piriformospora indica* and *Magnaporthe oryzae*. Both fungi invaded mutant and wild type  
134 root tissue equivalently well (Supplemental Figure S2) suggesting that NOPE1 might be  
135 specifically required for interaction with AMF.

136

### 137 **Mutation of maize *NOPE1* recapitulates the AM phenotype of *Osnope1*.**

138 The maize *nope1* mutant arose in a *Mutator* mutagenized population<sup>16</sup>. Poor seed viability and  
139 suppression of the phenotype of the original allele prevented further characterization of the maize  
140 *nope1* mutation; instead, we undertook a reverse genetics approach to verify the role of the maize  
141 homologue of *OsNOPE1* in AM symbiosis. The maize genome contains a single gene,  
142 *GRMZM2G176737*, showing high similarity to *OsNOPE1* (BLASTP; score=488, ID=83%, e-  
143 value=8.2xe<sup>-61</sup>). *GRMZM2G176737* is located on Chromosome 10 near to the original mapped  
144 position of the *nope1* mutation (Figure 1A, underlined). To determine the role of  
145 *GRMZM2G176737* during AM symbiosis, a *Dissociation (Ds)*-tagged maize population was  
146 screened for transposon insertions at this locus<sup>23,24</sup>. A *Ds* element was identified that had inserted

147 within the first exon at 600 bp downstream of ATG, resulting in disruption of gene function as  
148 reflected by the lack of corresponding transcript accumulation (Figure 3B). Microscopic  
149 inspection of inoculated maize roots confirmed that despite fungal proliferation on the mutant root  
150 surface the hyphae were septated. Hyphopodia were malformed and failed to penetrate while wild  
151 type roots supported extensive development of intraradical fungal structures (Figure 3C and D).  
152 Quantification of intraradical fungal structures revealed significantly lower fungal colonization of  
153 homozygous individuals ( $p < 0.05$ ) as compared to the wild-type (Figure 3E). Also transcript  
154 levels of the maize homologues of the rice AM marker genes *OsAM3*<sup>21</sup> and *OsPT11*<sup>25</sup>,  
155 *GRMZM2G135244* (*ZmAM3*) and *GRMZM5G881088* (*ZmPT6*)<sup>26</sup>, were lower in inoculated roots  
156 homozygous for the transposon insertion as compared to hemizygous and wild-type siblings  
157 (Figure 3F).

158       Reproduction of compromised early AMF-interaction of the original *nope1* mutant<sup>16</sup> in both  
159 loss of function alleles of rice *LOC\_Os04g01520* (*OsNOPE1*) and maize *GRMZM2G176737*  
160 (*ZmNOPE1*) strongly indicates that *GRMZM2G176737* and *LOC\_Os04g01520* correspond to the  
161 *NOPE1* gene.

162

163 **NOPE1 belongs to the Major Facilitator Superfamily and occurs in all land plant species.**

164 Computational analysis of protein topology (<http://phobius.binf.ku.dk/>) and domains  
165 (<http://smart.embl-heidelberg.de/>) predicted that NOPE1 has 12 transmembrane domains, no  
166 signal peptide and contains a domain of unknown function, DUF895, between amino acids 49 and  
167 181 (Supplemental Figure S3A). The NOPE1 protein is predicted to belong to the Major  
168 Facilitator Superfamily (MFS, Pfam e-value 4.9e-13) of membrane transport proteins, thereby  
169 suggesting NOPE1 to be involved in the transport of small molecules across membranes.

170       Blast Search based on available sequence data (<http://blast.ncbi.nlm.nih.gov/Blast.cgi>),  
171 indicated that genes encoding NOPE1 are present in the genomes of all land plants investigated,

172 including non-mycorrhizal plant species (Supplemental Figure S3B). The genome of the model  
173 legume *Medicago truncatula* contains two copies of *NOPE1* orthologs; *MtNOPE1a*  
174 (*Medtr3g093270*) and *MtNOPE1b* (*Medtr3g093290*) and the corresponding gene products share  
175 63% identity (79% positive) and 64% identity (81% positive), respectively with OsNOPE1,  
176 providing a plausible explanation for the lack of recovery of *NOPE1*-associated AM phenotypes  
177 from forward genetic screens in legumes. The model plant *Arabidopsis thaliana* is unable to form  
178 AM symbiosis, but yet two *NOPE1* orthologs *At1g18000* and *At1g18010* are present. At the  
179 genomic level, the two genes are identical in DNA, and protein sequence and share 57% identity  
180 (71% positive) at the protein level with rice NOPE1, indicating that the protein serves functions  
181 beyond AM symbiosis. The Arabidopsis electronic Fluorescent Pictograph indicated that both  
182 Arabidopsis genes are expressed constitutively throughout the plant with highest transcript  
183 accumulation in cauline leaves and flowers <https://bar.utoronto.ca/eplant/><sup>27</sup>. To determine a  
184 possible role of the Arabidopsis *NOPE1* genes for overall plant development, RNAi-based  
185 silencing lines were generated that targeted both genes simultaneously. We selected line  
186 *AtMNC42* and *AtMNC58* which displayed the strongest down-regulation for both genes  
187 (Supplemental Figure S4A) but were unable to find evidence for any altered developmental  
188 phenotype when inspecting germination, root and shoot architecture, flowering and seed setting.

189

#### 190 **Rice NOPE1 mediates N-acetylglucosamine transport in *Candida albicans*.**

191 In order to investigate the mechanism by which NOPE1 influences AM symbioses, we sought to  
192 identify putative homologs with functional annotation. As no land plant orthologs had been  
193 previously functionally characterised, we adopted a reciprocal best hit (RBH) strategy between  
194 *Oryza sativa* and the human pathogenic fungus *Candida albicans*. RBH identified the functionally  
195 characterised protein Ng1 as a putative orthologue of NOPE1 (41% identity and 59% positive).  
196 Ng1 mediates N-acetylglucosamine (GlcNAc) transport across the plasma membrane of *C.*

197 *albicans*, enabling growth on GlcNAc as the only source of carbohydrates<sup>28</sup>. A key feature of the  
198 *C. albicans* virulence is the cells' ability to reversibly shift from isotropic budding to polarized  
199 filamentous growth in response to environmental signals<sup>29</sup>. Amongst the stimuli triggering this  
200 morphological switch is GlcNAc, which induced filamentous hyphal growth<sup>30</sup>. Deletion of *NGT1*  
201 impairs *C. albicans* GlcNAc uptake, preventing cells from switching morphology and from  
202 proliferating on GlcNAc-containing medium<sup>17,31</sup>. To address whether OsNOPE1 is a functional  
203 GlcNAc transporter, a *C. albicans* codon-optimized version of the rice *OsNOPE1*, driven by the  
204 native fungal *NGT1* promoter was transformed into the *C. albicans* mutant *ngt1Δ*. Remarkably,  
205 three different assays demonstrated that rice *OsNOPE1* restored the function of can complement *C.*  
206 *albicans ngt1Δ* cells (Figure 4A-C): the expression of *OsNOPE1* restored the ability of the *ngt1Δ*  
207 mutant *C. albicans* to grow on GlcNAc medium, to undergo filamentous hyphal differentiation  
208 upon GlcNAc treatment, and to take up radioactive GlcNAc from the medium. Rice *OsNOPE1*  
209 therefore mediated GlcNAc uptake in *C. albicans*, indicating functional conservation of the  
210 protein across plant and fungal kingdoms.

211 In order to determine substrate specificity of OsNOPE1 with regard to transport of other related  
212 hexose sugars, competition assays were performed in which an excess of cold hexoses was  
213 provided together with [<sup>3</sup>H]GlcNAc. Control studies showed that the addition of a 2-fold excess of  
214 cold GlcNAc led to a partial decline in the uptake of radioactive GlcNAc and there was nearly  
215 complete inhibition at 20-fold excess cold GlcNAc (Supplemental Figure S5). OsNOPE1 showed  
216 strong specificity for transporting GlcNAc, since a 200-fold excess of glucosamine, dextrose,  
217 fructose or galactose did not significantly impact on the amount of [<sup>3</sup>H]GlcNAc transported into  
218 the cells. A 200-fold excess of N-acetylmannosamine partially competed with [<sup>3</sup>H]GlcNAc ( $p <$   
219 0.01 by non-parametric one way ANOVA), suggesting that the N-acetyl moiety may be important  
220 for transport substrate specificity. Overall, these results demonstrated that OsNOPE1 exhibits a  
221 high specificity for transporting GlcNAc, similar to *C. albicans* Ngt1 (Supplemental Figure S5).

222

223 **NOPE1 mediates N-acetylglucosamine influx in plants.**

224 The efficient rice NOPE1 transport activity in *C. albicans* predicted that OsNOPE1 may  
225 mediate GlcNAc transport across the plasma membrane also in plants. We verified subcellular  
226 localization of At1g18000 in stably transformed *A. thaliana* plants by using the constitutively  
227 active Arabidopsis ubiquitin promoter to express the in-frame fused *YFP-AtNOPE1a*. Three  
228 independent lines were analyzed to determine reproducible localization patterns. Propidium iodide  
229 was applied to counterstain the plant cell wall. **Transgenic lines showed a reproducible and clear**  
230 **signal consistent with plasma membrane localization, here shown for line At4731y-4, (Figure 5A).**  
231 It is therefore conceivable that absence of the NOPE1 transport activity at the plasma membrane  
232 leads to the early AM phenotype of the rice and maize *nope1* mutants.

233 To confirm that OsNOPE1 can transport GlcNAc in its native plant environment, we measured  
234 [<sup>3</sup>H]GlcNAc root uptake in rice seedlings<sup>32</sup> over time using wild type, *OsNOPE1* and the  
235 genetically complemented mutant line C4. While the uptake rates observed for the wild type and  
236 the complemented C4 line were 2.37 ( $R^2 = 0.992$ ) and 2.00 pmol ( $R^2 = 0.991$ ) [<sup>3</sup>H]GlcNAc/60 min  
237 and plant, respectively, that of the *Osnope1* mutant was 0.624 pmol ( $R^2 = 0.960$ ) [<sup>3</sup>H]GlcNAc /60  
238 min and plant, thus significantly slower ( $p < 0.05$ ; Figure 5B). To test if NOPE1 supported  
239 transport of GlcNAc across plant cell membranes in another system, we measured the  
240 [<sup>3</sup>H]GlcNAc uptake in protoplasts derived from the *A. thaliana* At1g18000 overexpression line,  
241 At4731y-4 and compared this uptake to that of the RNAi-silencing line AtMNC58 (Supplemental  
242 Figure S6). Uptake of [<sup>3</sup>H]GlcNAc displayed a linear increase over time and reached significantly  
243 higher uptake rates in the overexpression line At4731y-4 with  $2 \pm 0.05$  pmol [<sup>3</sup>H]GlcNAc/g  
244 chlorophyll at 25 min ( $p < 0.01$ ) as compared to  $1.25 \pm 0.1$  pmol [<sup>3</sup>H]GlcNAc/g chlorophyll  
245 acquired by protoplasts of the RNAi-silenced line AtMNC58 (Supplemental Figure S6). **Please**  
246 **note that the 0.5 min value does not correspond to specific uptake but to unspecific adsorption of**

247 **medium to the protoplasts.** Taken together, NOPE1 mediated GlcNAc uptake in whole roots and  
248 leaf protoplasts of mycorrhizal and non-mycorrhizal plant species, respectively.

249 **In addition, we quantified GlcNAc efflux in the rice seedling system.** Roots of wild type rice  
250 seedlings were first loaded by incubation with 100  $\mu\text{M}$  [ $^3\text{H}$ ]GlcNAc and then transferred to a  
251 solution either containing unlabeled GlcNAc at 50X concentration or no GlcNAc. Monitoring the  
252 levels of [ $^3\text{H}$ ]GlcNAc retained in the roots revealed that in both cases GlcNAc was released from  
253 the roots, but that at shorter times, significantly less ( $p < 0.05$ ) remained in the roots when the  
254 external medium contained no GlcNAc ( $2.21 \pm 0.10$  [ $^3\text{H}$ ]GlcNAc/plant) relative to roots incubated  
255 in high GlcNAc medium ( $3.30 \pm 0.36$  [ $^3\text{H}$ ]GlcNAc/plant, Figure 5C), indicating that substrate  
256 availability at the external side partially inhibited efflux.

257 **In summary, NOPE1 mediated GlcNAc uptake into plant cells, which conceivably also**  
258 **facilitated GlcNAc efflux across the plasma membrane, however export might be catalyzed by**  
259 **additional or alternative transporters.**

260

#### 261 **Distinct transcriptional responses of *R. irregularis* to rice wild type and *nope1* root exudates.**

262 The NOPE1-mediated GlcNAc transport across the plasma membrane may be required for  
263 symbiosis establishment by contributing to plant perception of AMF. AM specific marker genes  
264 from rice offer sensitive diagnostics and are routinely used to molecularly phenotype distinct  
265 stages of the interaction in rice<sup>21,33-37</sup>. Examining the mRNA levels of four AM marker genes  
266 (*AMI*, *AM3*, *AM14* and *PT11*) in control and inoculated wild type and *Osnope1* roots  
267 demonstrated that in the mutant these genes exhibited about two order of magnitude lower  
268 induction than in the wild type (Figure 5D). The low marker gene expression levels correlated  
269 with the low colonization level (Figure 2A). **However, the mutant may alternatively be affected in**  
270 **the uptake of compounds whose signaling functions are not monitored by these marker genes.**

271 An equally plausible scenario could be that NOPE1 function is required for the release of  
272 compounds that activate AMF towards symbiosis. As diffusible compounds released by plant  
273 roots such as SLs alter hyphal branching patterns<sup>8,9</sup>, we used *Gigaspora rosea* to assess hyphal  
274 ramification upon treatment with plant exudates. No difference was found in the number of hyphal  
275 apices and overall hyphal growth behaviour in response to exudates from wild type and *Osnope1*  
276 (Supplemental Figure S7). This is consistent with GlcNAc belonging to another chemical  
277 compound class than SLs, 2-OH fatty acids or flavonoids which trigger specific hyphal growth  
278 patterns (for review see<sup>1</sup>).

279 To more sensitively and comprehensively examine possible fungal responses to root-released  
280 compounds, RNAseq analysis was performed on pre-germinated *R. irregularis* spores exposed to  
281 either rice wild type or *Osnope1* root exudates at 1h, 24h and 7 days post treatment. Significantly  
282 differentially expressed genes (d.e.) between treatment and mock condition were defined by False  
283 Discovery Rate (FDR)  $\leq 0.05$ . Remarkably, wild-type vs mutant exudate treatment resulted in a  
284 much larger number of d.e. genes at 1h post treatment, corresponding to 1249 vs 388 genes,  
285 respectively, whereas the volume of the transcriptional response was more comparable at later  
286 time points (Table 1A and B). Next, we compared the d.e. gene lists of the two treatments at each  
287 time point and applied a 2-fold cut-off [Fold Change (FC)  $\geq 2$ ] (Table 2A). Treatment with wild-  
288 type exudates led to the induction of 92 genes at 1h, which were not induced when the fungus was  
289 exposed to *Osnope1* root exudates (Figure 6A top and bottom, Table 2A). At 24h and 7d treatment  
290 with wild-type exudates resulted in the induction of 283 and 901 genes, respectively (Figure 6A  
291 top, Table 2A and B). In contrast, although *Osnope1* exudate treatment induced 343 genes at 24h,  
292 only 256 genes had increased transcript levels at 7d (Figure 6A top and bottom, Table 2A and B).  
293 Therefore, exposure to wild-type and *Osnope1* exudates led to distinctly different transcriptional  
294 response patterns in the fungus. Time resolved gene ontology (GO) analysis on those genes which  
295 met the filtering criteria of FDR  $< 0.05$  and FC  $> 2$  (Table 2A and B), revealed an

296 overrepresentation of genes associated with the GO terms protein kinase and ATPase activity  
297 amongst the 92 d.e. genes (Figure 6B, Table 3A) suggesting an early induction of fungal signaling  
298 activities. At 24h either treatment had led to a significant change in the fungal transcriptome  
299 (Table 2A and B), however GO analysis suggested that while the fungus switched to an elevated  
300 oxidative status in response wild-type exudates, it induced stress responses upon mutant exudate  
301 treatment (Table 3B). While the ‘stress response signature’ remained for the fungal transcriptome  
302 at 7d post treatment with mutant root exudate, exposure to wild-type exudates induced fungal  
303 genes, associated with GO terms corresponding to a higher energetic and metabolic status (Figure  
304 6B, Table 3C). Together these data are consistent with an early and transient activation of fungal  
305 signaling, followed by the activation of genes involved in primary metabolism in wild type but not  
306 *Osnope1* root exudate treated fungus.

307 RNAseq results were validated by qRT-PCR analysis on a subset of representative d.e. genes  
308 using two selection criteria: (1) predicted to encode proteins with a potential role in processes  
309 involved in the initial recognition and interaction with the host plant (cell wall modification,  
310 transport, signaling) and (2) showing pronounced differences in the level of transcript  
311 accumulation at both 1h and 24h (Supplemental Figure S8A-C), only at 24h (Supplemental Figure  
312 S8D and E), and at 7 days (Supplemental Figure S8F and G). Interestingly, the *R. irregularis*  
313 *NGTI* homologue MIX9501\_16\_76<sup>38</sup> displayed a basal expression level throughout the  
314 experiment (Gene Expression Omnibus, accession n° GSE65595), and was not induced in  
315 response to treatment with either exudates or by GlcNAc treatments (Supplemental Figure S9).  
316 The specific fungal transcriptional response to rice wild type root exudates is consistent with the  
317 hypothesis that the NOPE1 function leads to adequate reprogramming of *R. irregularis* for host  
318 colonization. However, application of GlcNAc to *R. irregularis*-inoculated *Osnope1* mutant plants  
319 for seven weeks at 1 mM, 10 mM or 100 mM GlcNAc did not complement the mutant phenotype.  
320 This may be due to application of GlcNAc outside the biologically active concentration, or that

321 either the development of a GlcNAc gradient or efflux of a GlcNAc-conjugate might be necessary  
322 for stimulating the fungus.

323 On the assumption that wild type roots release the critical GlcNAc compound, we examined  
324 whether the presence of wild type exudates would restore AM colonization of the mutant when  
325 cocultivated within the same container. Indeed, roots of *Osnopel* were fully colonized when  
326 grown together with wild type but not with mutant ‘donor’ plants (Supplemental Figure S10),  
327 lending further support for NOPE1 being directly or indirectly required for the root exudation of  
328 an AMF activating compound.

329

### 330 **Discussion**

331 We report here the discovery of NOPE1 as a plasma membrane GlcNAc transporter required for  
332 the initiation of AM symbiosis in rice and maize. Current knowledge of the molecular  
333 mechanisms that plants employ to attract and reprogram mutualistic AMF in the rhizosphere is  
334 largely limited to the stimulatory effects that SLs exert on fungal metabolism and development. It  
335 has been anticipated that additionally secreted bioactive molecules are necessary to stimulate the  
336 fungus for symbiosis (<sup>39</sup>, for review see <sup>1</sup>). While there was no difference in the ability to induce  
337 pre-symbiotic hyphal branching, wild-type and *Osnopel* root exudates triggered distinct  
338 transcriptional responses in the fungus. After 1h exposure to wild type exudates, transcripts  
339 assigned to GO terms associated with signaling functions were induced, consistent with the  
340 conditioning of the fungus by the plant prior to contact formation. This hypothesis was further  
341 supported by the restoration of normal levels of colonization of *Osnopel* by co-cultivation with  
342 wild-type plants, indicative for bioactive molecules in the wild-type exudates. We therefore  
343 hypothesize that NOPE1 fulfills distinct roles, complementary to SL, in stimulating the fungus for  
344 the interaction.

345 NOPE1 represents a functional GlcNAc transporter and mediates efficient GlcNAc import in  
346 *C. albicans*, rice and Arabidopsis. GlcNAc occurs prevalently in microbial environments as a  
347 building unit of either fungal and bacterial cell walls or of microbial signaling molecules such as  
348 rhizobial nod-factors. Whether GlcNAc uptake by the plant contributes to microbe perception or  
349 influences root exudate composition, e.g. via signaling remains at present unclear. Analysis of the  
350 expression of a small number of marker genes revealed quantitative differences between wild type  
351 and mutant that were proportional to the level of root colonization.

352 Wild-type roots were shown to be able to acquire and release GlcNAc; as uptake depended on  
353 functional NOPE1, efflux might also require NOPE1. However, the chemical identity of the  
354 bioactive molecule is at present unknown as addition of GlcNAc to inoculated mutant plants did  
355 not recover wild-type colonization levels. At this stage, the biological role of NOPE1 in the  
356 release of bioactive compounds into the rhizosphere remains to be determined.

357 Plants produce detectable quantities of cellular GlcNAc; mass spectrometry-based analysis  
358 detected abundant levels of GlcNAc monomers in leaves of wild type *Arabidopsis thaliana*<sup>40</sup>.  
359 Even though corresponding data are not available from roots a similar scenario can be expected  
360 due to the important intracellular roles GlcNAc plays in e.g. the posttranslational modification of  
361 lipids and proteins or also in influencing diverse cellular processes as glycans. For example  
362 interference with biosynthesis of the activated substrate for GlcNAc transfer, UDP-GlcNAc, in  
363 rice roots impaired cell expansion in the root elongation zone, leading to a short root phenotype,  
364 thereby demonstrating the importance of the GlcNAc metabolism for root functioning<sup>41</sup>.

365 Host-secreted GlcNAc is known to act as a potent signaling molecule for a number of  
366 microbial organisms including the facultative human pathogenic fungus *C. albicans*<sup>18</sup>. Exposure  
367 to GlcNAc leads to the induction of invasive hyphal growth and the expression of virulence genes  
368 such as the adhesins that facilitate attachment to host cells (for review see<sup>28</sup>). Also the thermally  
369 dimorphic pathogenic fungi *Histoplasma capsulatum* and *Blastomyces dermatitidis* respond to

370 treatment with GlcNAc by a similar yeast-to-filament switch <sup>42</sup>. In these facultative human  
371 pathogens GlcNAc additionally functions as a source of sugar. The utilization of plant-derived  
372 GlcNAc as a substrate was recently reported for the plant-pathogenic bacteria *Xanthomonas*  
373 *campestris* pv. *campestris* while infecting leaves of *Brassica oleracea* <sup>43</sup>. In these bacteria,  
374 availability of GlcNAc-containing compounds induces numerous bacterial glycosyl hydrolases,  
375 which enzymatically release *N*-glycans from extracellular plant *N*-glycosylated proteins. The  
376 closely related vector-borne phytopathogenic bacterium *Xylella fastidiosa* enzymatically digests  
377 GlcNAc polymers (chitin) available in the foregut of the insect vector and also uses the acquired  
378 GlcNAc as a nutrient source <sup>44</sup>. Remarkably, the effects of host-provided GlcNAc on microbial  
379 physiology extend towards the mutualistic bioluminescent squid-vibrio model where host-derived  
380 GlcNAc mono- and dimers act as a regulators of shifting the bacterial metabolism to provide  
381 optimal symbiont services to the host <sup>45</sup>.

382 Our study identifies the first GlcNAc transporter in plants and introduces the importance of  
383 NOPE1 in interspecies communication between rice and *R. irregularis*, thereby suggesting  
384 NOPE1 to represent an evolutionarily ancient and ecologically prevalent protein for the interaction  
385 with Glomeromycotan fungi.

386

387

## 388 **References**

- 389 1 Nadal, M. & Paszkowski, U. Polyphony in the rhizosphere: presymbiotic communication in  
390 arbuscular mycorrhizal symbiosis. *Curr Opin Plant Biol* **16**, 473-479, doi:10.1016/j.pbi.2013.06.005  
391 (2013).
- 392 2 Oldroyd, G. E. Speak, friend, and enter: signalling systems that promote beneficial symbiotic  
393 associations in plants. *Nat Rev Microbiol* **11**, 252-263, doi:10.1038/nrmicro2990 (2013).
- 394 3 Gutjahr, C. & Parniske, M. Cell and developmental biology of arbuscular mycorrhiza symbiosis.  
395 *Annual review of cell and developmental biology* **29**, 593-617, doi:10.1146/annurev-cellbio-  
396 101512-122413 (2013).
- 397 4 Miyata, K. *et al.* The bifunctional plant receptor, OsCERK1, regulates both chitin-triggered  
398 immunity and arbuscular mycorrhizal symbiosis in rice. *Plant Cell Physiol* **55**, 1864-1872,  
399 doi:10.1093/pcp/pcu129 (2014).

400 5 Zhang, X. *et al.* The receptor kinase CERK1 has dual functions in symbiosis and immunity  
401 signalling. *Plant J* **81**, 258-267, doi:10.1111/tpj.12723 (2015).

402 6 Gutjahr, C. *et al.* Rice perception of symbiotic arbuscular mycorrhizal fungi requires the karrikin  
403 receptor complex. *Science* **350**, 1521-1524 (2015).

404 7 Bécard, G., Douds, D. D. & Pfeffer, P. E. Extensive In Vitro Hyphal Growth of Vesicular-Arbuscular  
405 Mycorrhizal Fungi in the Presence of CO<sub>2</sub> and Flavonols. *Appl Environ Microbiol* **58**, 821-825  
406 (1992).

407 8 Nagahashi, G. & Douds, D. D., Jr. The effects of hydroxy fatty acids on the hyphal branching of  
408 germinated spores of AM fungi. *Fungal biology* **115**, 351-358, doi:10.1016/j.funbio.2011.01.006  
409 (2011).

410 9 Akiyama, K., Matsuzaki, K. & Hayashi, H. Plant sesquiterpenes induce hyphal branching in  
411 arbuscular mycorrhizal fungi. *Nature* **435**, 824-827 (2005).

412 10 Besserer, A., Becard, G., Jauneau, A., Roux, C. & Sejalón-Delmas, N. GR24, a synthetic analog of  
413 strigolactones, stimulates the mitosis and growth of the arbuscular mycorrhizal fungus *Gigaspora*  
414 *rosea* by boosting its energy metabolism. *Plant Physiol* **148**, 402-413, doi:pp.108.121400 [pii]  
415 10.1104/pp.108.121400 (2008).

416 11 Besserer, A. *et al.* Strigolactones stimulate arbuscular mycorrhizal fungi by activating  
417 mitochondria. *PLoS Biol* **4**, e226 (2006).

418 12 Gomez-Roldán, V. *et al.* Strigolactone inhibition of shoot branching. *Nature* **455**, 189-194,  
419 doi:nature07271 [pii]  
420 10.1038/nature07271 (2008).

421 13 Bécard, G., Taylor, L., Jr, D. D., Pfeffer, P. & Doner, L. Flavonoids are not necessary plant signals in  
422 arbuscular mycorrhizal symbiosis. *Molecular Plant Microbe Interaction* **8**, 252-258 (1995).

423 14 Wang, E. *et al.* A Common Signaling Process that Promotes Mycorrhizal and Oomycete  
424 Colonization of Plants. *Curr Biol* **22**, 2242-2246, doi:10.1016/j.cub.2012.09.043 (2012).

425 15 Wewer, V., Brands, M. & Dormann, P. Fatty acid synthesis and lipid metabolism in the obligate  
426 biotrophic fungus *Rhizophagus irregularis* during mycorrhization of *Lotus japonicus*. *Plant J* **79**,  
427 398-412, doi:10.1111/tpj.12566 (2014).

428 16 Paszkowski, U., Jakovleva, L. & Boller, T. Maize mutants affected at distinct stages of the  
429 arbuscular mycorrhizal symbiosis. *Plant J.* **47**, 165-173 (2006).

430 17 Alvarez, F. J. & Konopka, J. B. Identification of an N-acetylglucosamine transporter that mediates  
431 hyphal induction in *Candida albicans*. *Molecular biology of the cell* **18**, 965-975,  
432 doi:10.1091/mbc.E06-10-0931 (2007).

433 18 Naseem, S. & Konopka, J. B. N-acetylglucosamine Regulates Virulence Properties in Microbial  
434 Pathogens. *PLoS pathogens* **11**, e1004947, doi:10.1371/journal.ppat.1004947 (2015).

435 19 Güimil, S. *et al.* Comparative transcriptomics of rice reveals an ancient pattern of response to  
436 microbial colonization. *Proc Natl Acad Sci* **102**, 8066-8070 (2005).

437 20 Jeong, D. H. *et al.* Generation of a flanking sequence-tag database for activation-tagging lines in  
438 japonica rice. *Plant J* **45**, 123-132 (2006).

439 21 Gutjahr, C. *et al.* Arbuscular mycorrhiza-specific signaling in rice transcends the common  
440 symbiosis signaling pathway. *Plant Cell* **20**, 2989-3005, doi:tpc.108.062414 [pii]  
441 10.1105/tpc.108.062414 (2008).

442 22 Marcel, S., Sawers, R., Oakeley, E., Angliker, H. & Paszkowski, U. Tissue-adapted invasion  
443 strategies of the rice blast fungus *Magnaporthe oryzae*. *Plant Cell* **22**, 3177-3187,  
444 doi:tpc.110.078048 [pii]  
445 10.1105/tpc.110.078048 (2010).

446 23 Ahern, K. R. *et al.* Regional mutagenesis using Dissociation in maize. *Methods* **49**, 248-254,  
447 doi:S1046-2023(09)00092-9 [pii]

448 10.1016/j.ymeth.2009.04.009 (2009).

449 24 Vollbrecht, E. *et al.* Genome-wide distribution of transposed Dissociation elements in maize. *Plant*  
450 *Cell* **22**, 1667-1685, doi:tpc.109.073452 [pii]

451 10.1105/tpc.109.073452 (2010).

452 25 Paszkowski, U., Kroken, S., Roux, C. & Briggs, S. Rice phosphate transporters include an  
453 evolutionarily divergent gene specifically activated in arbuscular mycorrhizal symbiosis. *Proc Natl*  
454 *Acad Sci* **99**, 13324-13329 (2002).

455 26 Nagy, R. *et al.* Differential regulation of five Pht1 phosphate transporters from maize (*Zea mays*  
456 L.). *Plant Biol.* **8**, 186-197 (2006).

457 27 Winter, D. *et al.* An "Electronic Fluorescent Pictograph" browser for exploring and analyzing large-  
458 scale biological data sets. *PLoS One* **2**, e718, doi:10.1371/journal.pone.0000718 (2007).

459 28 Konopka, J. B. N-acetylglucosamine (GlcNAc) functions in cell signaling. *Scientifica (Cairo)* **2012**,  
460 doi:10.6064/2012/489208 (2012).

461 29 Whiteway, M. & Oberholzer, U. Candida morphogenesis and host-pathogen interactions. *Current*  
462 *opinion in microbiology* **7**, 350-357, doi:10.1016/j.mib.2004.06.005 (2004).

463 30 Simonetti, N., Strippoli, V. & Cassone, A. Yeast-mycelial conversion induced by N-acetyl-D-  
464 glucosamine in *Candida albicans*. *Nature* **250**, 344-346 (1974).

465 31 Naseem, S., Gunasekera, A., Araya, E. & Konopka, J. B. N-acetylglucosamine (GlcNAc) induction of  
466 hyphal morphogenesis and transcriptional responses in *Candida albicans* are not dependent on its  
467 metabolism. *The Journal of biological chemistry* **286**, 28671-28680, doi:10.1074/jbc.M111.249854  
468 (2011).

469 32 Yamada, K. *et al.* Monosaccharide absorption activity of Arabidopsis roots depends on expression  
470 profiles of transporter genes under high salinity conditions. *The Journal of biological chemistry*  
471 **286**, 43577-43586, doi:10.1074/jbc.M111.269712 (2011).

472 33 Gutjahr, C. *et al.* The half-size ABC transporters STR1 and STR2 are indispensable for mycorrhizal  
473 arbuscule formation in rice. *Plant J* **69**, 906-920, doi:10.1111/j.1365-313X.2011.04842.x (2012).

474 34 Gutjahr, C. *et al.* Transcriptome diversity among rice root types during asymbiosis and interaction  
475 with arbuscular mycorrhizal fungi. *Proc Natl Acad Sci U S A* **112**, 6754-6759,  
476 doi:10.1073/pnas.1504142112 (2015).

477 35 Mukherjee, A. & Ane, J. M. Germinating spore exudates from arbuscular mycorrhizal fungi:  
478 molecular and developmental responses in plants and their regulation by ethylene. *Mol Plant*  
479 *Microbe Interact* **24**, 260-270, doi:10.1094/MPMI-06-10-0146 (2011).

480 36 Yang, S. Y. *et al.* Nonredundant regulation of rice arbuscular mycorrhizal symbiosis by two  
481 members of the phosphate transporter1 gene family. *Plant Cell* **24**, 4236-4251,  
482 doi:10.1105/tpc.112.104901 (2012).

483 37 Yoshida, S. *et al.* The D3 F-box protein is a key component in host strigolactone responses  
484 essential for arbuscular mycorrhizal symbiosis. *New Phytol* **196**, 1208-1216, doi:10.1111/j.1469-  
485 8137.2012.04339.x (2012).

486 38 Kobae, Y. *et al.* Up-regulation of genes involved in N-acetylglucosamine uptake and metabolism  
487 suggests a recycling mode of chitin in intraradical mycelium of arbuscular mycorrhizal fungi.  
488 *Mycorrhiza* **25**, 411-417, doi:10.1007/s00572-014-0623-2 (2015).

489 39 Gadkar, V. *et al.* Root exudate of pmi tomato mutant M161 reduces AM fungal proliferation in  
490 vitro. *FEMS microbiology letters* **223**, 193-198 (2003).

491 40 Vanholme, B. *et al.* Accumulation of N-acetylglucosamine oligomers in the plant cell wall affects  
492 plant architecture in a dose-dependent and conditional manner. *Plant Physiol* **165**, 290-308,  
493 doi:10.1104/pp.113.233742 (2014).

494 41 Jiang, H. *et al.* A novel short-root gene encodes a glucosamine-6-phosphate acetyltransferase  
495 required for maintaining normal root cell shape in rice. *Plant Physiol* **138**, 232-242,  
496 doi:10.1104/pp.104.058248 (2005).

497 42 Gilmore, S. A., Naseem, S., Konopka, J. B. & Sil, A. N-acetylglucosamine (GlcNAc) triggers a rapid,  
498 temperature-responsive morphogenetic program in thermally dimorphic fungi. *PLoS genetics* **9**,  
499 e1003799, doi:10.1371/journal.pgen.1003799 (2013).

500 43 Boulanger, A. *et al.* The plant pathogen *Xanthomonas campestris* pv. *campestris* exploits N-  
501 acetylglucosamine during infection. *MBio* **5**, e01527-01514, doi:10.1128/mBio.01527-14 (2014).

502 44 Killiny, N., Prado, S. S. & Almeida, R. P. Chitin utilization by the insect-transmitted bacterium  
503 *Xylella fastidiosa*. *Appl Environ Microbiol* **76**, 6134-6140, doi:10.1128/AEM.01036-10 (2010).

504 45 Pan, M., Schwartzman, J. A., Dunn, A. K., Lu, Z. & Ruby, E. G. A Single Host-Derived Glycan Impacts  
505 Key Regulatory Nodes of Symbiont Metabolism in a Coevolved Mutualism. *MBio* **6**, e00811,  
506 doi:10.1128/mBio.00811-15 (2015).

507

508

509

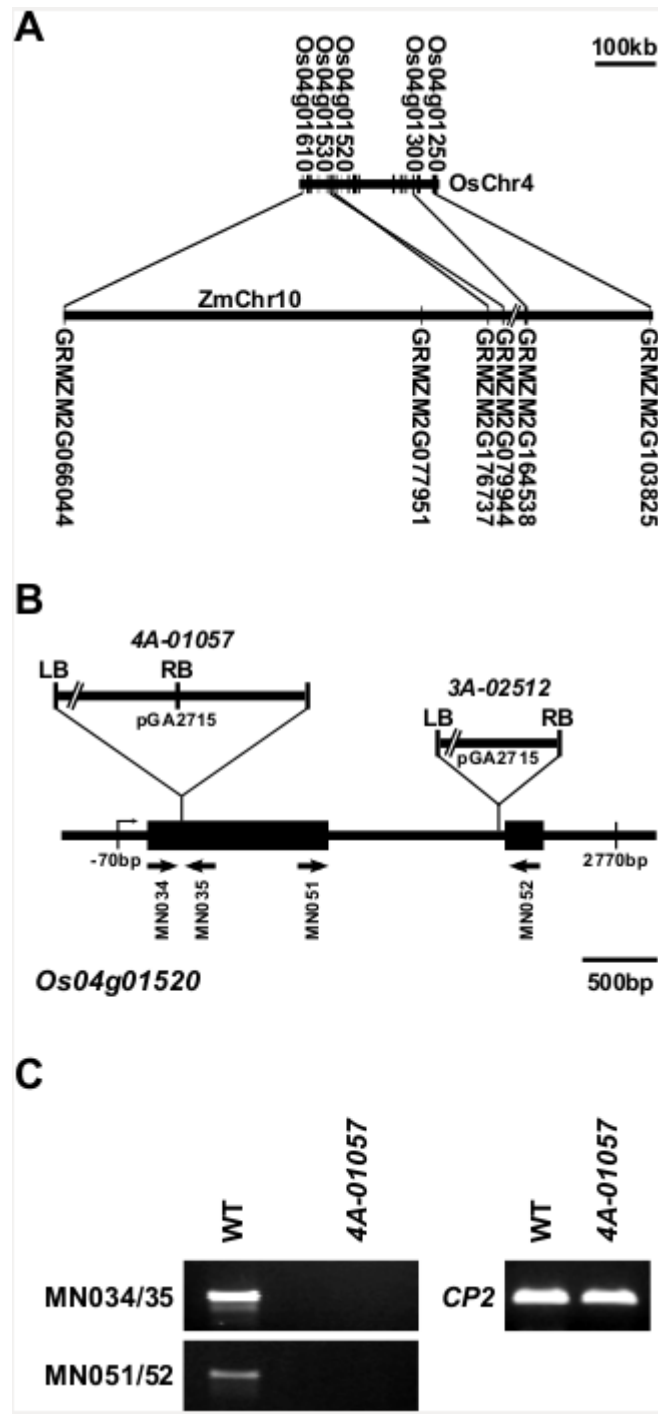
510 **Acknowledgements:** We kindly thank Jacqueline Gheyselinck and Anne Bates for their technical  
511 assistance. We are grateful to John Arbuckle (DuPont/Pioneer) for helping with mapping the  
512 maize *nope1* mutant and Sam Brockington for guidance with advanced BLAST searches.  
513 Research in the U.P. laboratories was supported by the Swiss National Science Foundation grants  
514 3100A0-104132, PP00A-110874, PP00P3-130704 and by the Gatsby Charitable Foundation grant  
515 RG60824. S.N and J.B.K were supported by a grant from the National Institutes of Health  
516 (R01GM116048).

517

518 **Author contribution:** M.N., R.S., N.G., E.M., J.B.K., T.P.B. and U.P. designed the experiments. M.N.,  
519 R.S., S.N., B.B., C.K., A.S., G.A., K.A., A.R., C.G., and C.R., performed the experiments. C.R. performed  
520 bioinformatics and statistical analyses of the RNAseq data. M.N., R.S., C.R., E.M., J.B.K. and U.P. wrote  
521 the manuscript.

522 *R. irregularis* RNAseq reads have been released at Gene Expression Omnibus (accession n°  
523 GSE65595). Correspondence and requests for materials should be addressed to U.P.  
524 (up220@cam.ac.uk). The authors declare no conflict of interest.

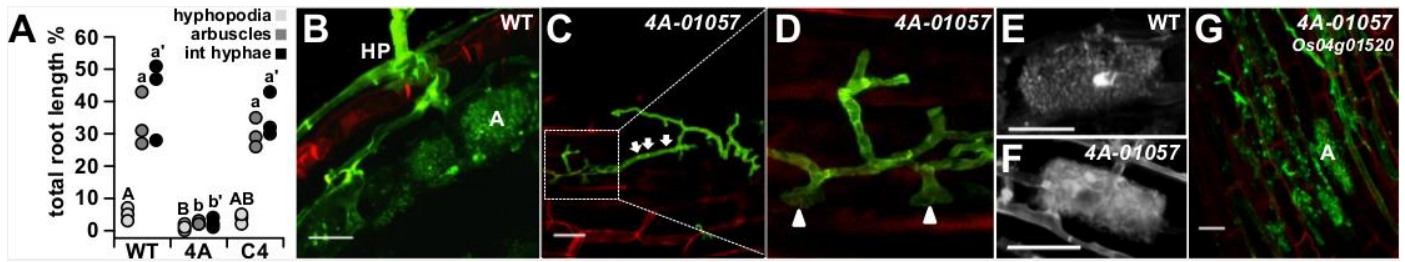
525



527 **Figure 1. Identification of syntenic rice and maize *NOPE1* candidate genes.** A, Physical map  
 528 of the *nope1* interval in syntenic regions of rice chromosome 4 (OsChr4) and maize chromosome  
 529 10 (ZmChr10). Maize and rice shown on a common scale with arrows indicating orientation.  
 530 Double bar indicates a break in the representation of the maize chromosome. Annotated gene  
 531 models are shown by bars and orthologous pairs connected with a dotted line. Only those rice  
 532 genes assigned orthologs in the maize region are labeled by name. Maize and rice *NOPE1*  
 533 homologs are indicated (underline). B, Structure of the rice gene *LOC\_Os04g01520* and position  
 534 of T-DNA insertions present in the lines in lines 4A-01057 and 3A-02512. Sites of transcriptional  
 535 initiation and termination are indicated relative to the start of translation, at -70bp and 2770bp,

536 respectively. Arrows represent primers used in C, RT-PCR-based analysis of *LOC\_Os04g01520*  
537 transcript levels in wild type (WT) and *4A-01057*. LB, left border; RB right border; *CP2*,  
538 *CYCLOPHILLIN* (*LOC\_Os02g02890*).

539 **FIGURE 2 (2 columns)**

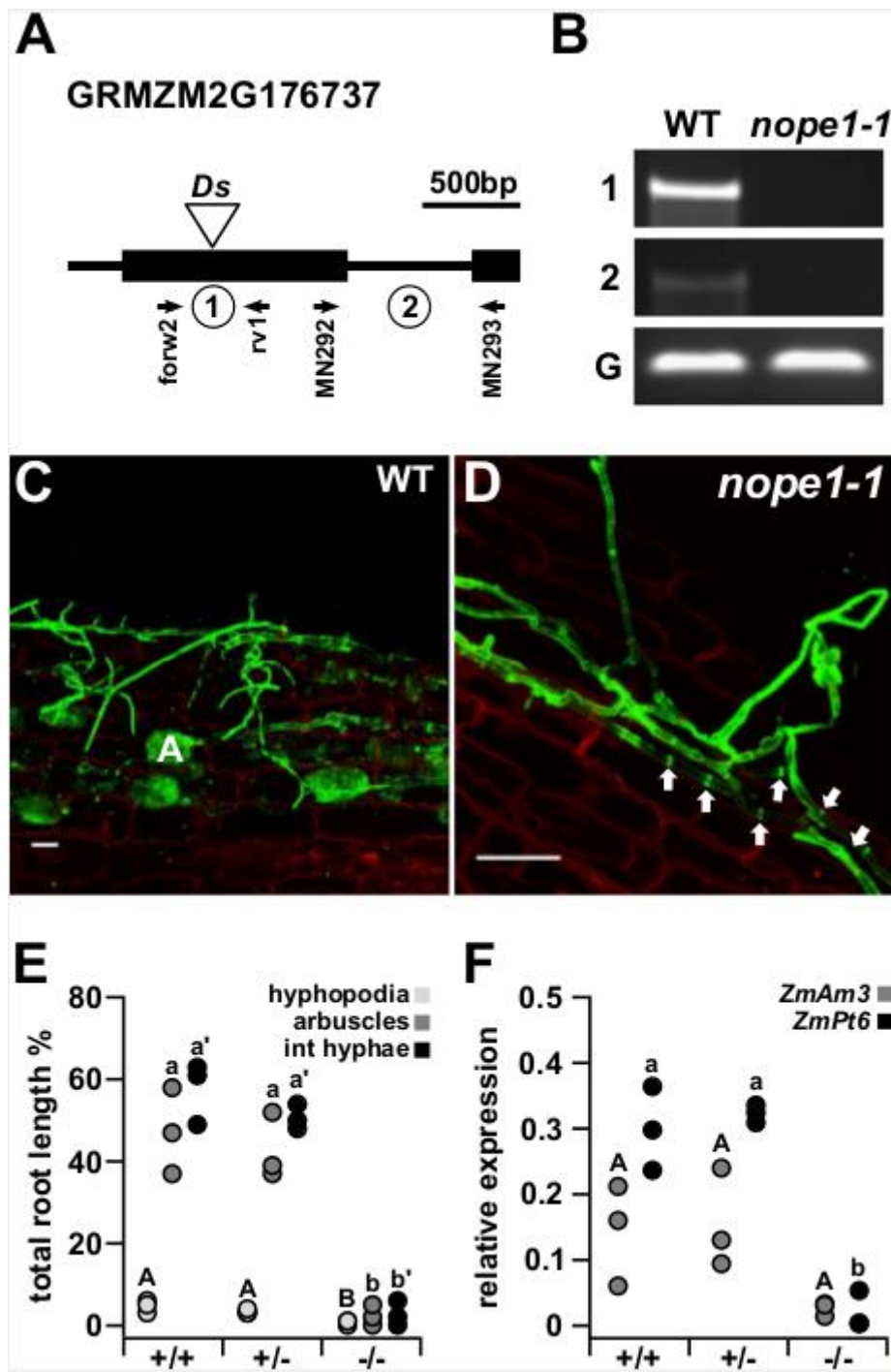


540

541 **Figure 2. Colonization by *R. irregularis* is disrupted in the rice insertion line 4A-01057.** **A,**  
 542 Percentage root length colonization in individuals segregating for the T-DNA insertion 4A-01057  
 543 at 6 wpi. Points represent individual plants. Means groups assigned for each fungal structure  
 544 indicated by letters (adj.  $p < 0.05$ ); **B-G,** WGA-staining of fungal structures and propidium-iodide  
 545 counterstained plant cell walls of rice roots inoculated with *R. irregularis* at 6wpi as examined by  
 546 laser scanning confocal microscopy. **B,** Hyphopodium (HP) and arbuscules differentiation in a  
 547 wild type (WT) root **C,** Misshapen and highly septate (arrows) hyphopodial hypha on the surface  
 548 of the root of a plant homozygous for the 4A-01057 insertion. **D,** Detail of hyphopodia on the  
 549 surface of the roots of a 4A-01057 homozygous plant, showing several aborted penetration  
 550 attempts (arrowhead). Morphologically equivalent arbuscules formed in the roots of wild type (**E**)  
 551 and 4A-01057 homozygous (**F**) plants. **G,** Arbuscules formed in root cortical cells of the  
 552 complemented line C4. HP, hyphopodium; A, arbuscule. scale bar = 50 $\mu$ m.

553

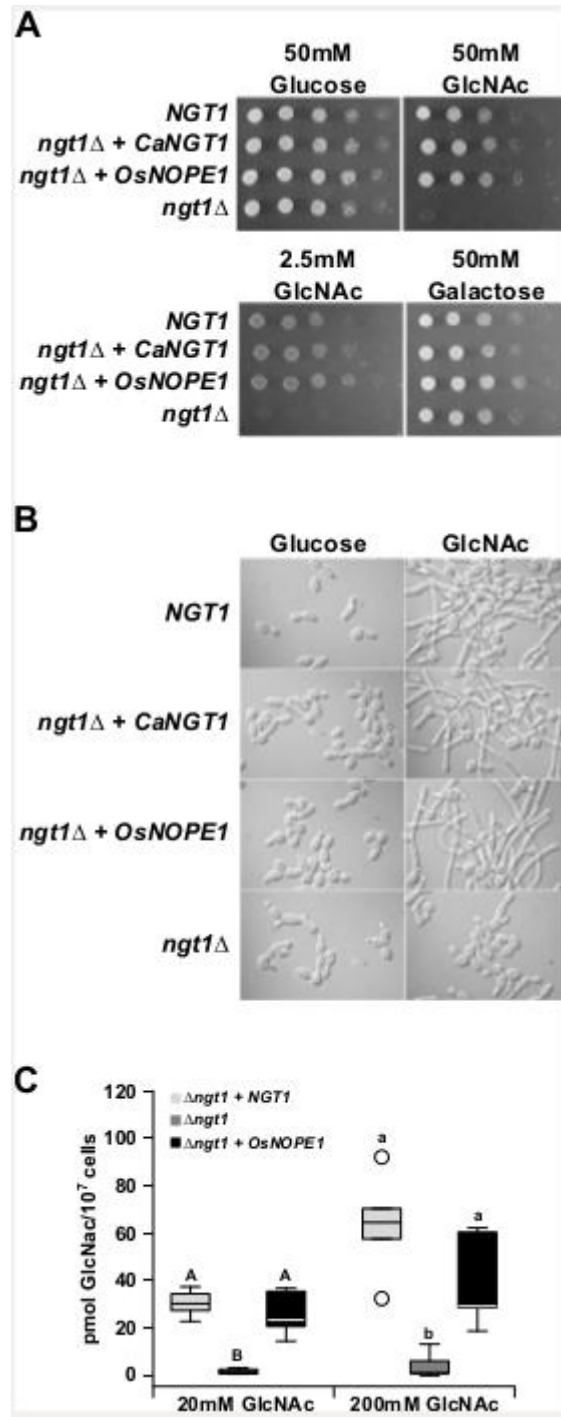
554



556 **Figure 3.** Mutation of the maize gene *GRMZM2G176737* reproduces the *Osnope1*  
 557 **phenotype.** **A**, *GRMZM2G176737* gene structure and position of *Ds* transposon insertion  
 558 (triangle). Arrows indicate position of primers used in **B**; forw2, ZmLph2-forw2; rv1, ZmLph2-  
 559 rv1 **B**, RT-PCR analysis of *GRMZM2G176737* transcript accumulation in the roots of plants  
 560 homozygous for the *Ds* insertion *GRMZM2G176737::Ds* using primers flanking (1) and  
 561 downstream (2) of the insertion site (reaction 1); *GAPDH*, *GLYCERALDEHYDE 3-PHOSPHATE*  
 562 *DEHYDROGENASE* (*GRMZM2G046804*). **C** and **D**, WGA-staining of fungal structures and  
 563 propidium-iodide counterstained plant cell walls of maize roots inoculated with *R. irregularis* at 6  
 564 wpi, as examined by laser scanning confocal microscopy. **C**, On wild type roots the fungus

565 develops normal hyphopodia and extensively colonizes the root forming frequent arbuscules. **D**, A  
566 hyphopodium on roots of *GRMZM2G176737::Ds* appears misshaped with multiple septa (arrows)  
567 and fails to penetrate the root tissue. A, arbuscule. Scale bar = 50µm. **E**, Percentage *R. irregularis*  
568 root length colonization of individuals segregating *GRMZM2G176737::Ds* at 6 wpi (+/+, wild  
569 type, +/-, heterozygote, -/- homozygous mutant). Points represent individual plants. Means groups  
570 were calculated *post hoc* independently for each structure and are indicated by letters ( $p < 0.05$ ). **F**,  
571 qRT-PCR-based analysis of transcript accumulation of *ZmAM3* (*GRMZM2G135244*) and *ZmPT6*  
572 (*GRMZM5G881088*) in maize plants segregating *GRMZM2G176737::Ds* at 6wpi with *R.*  
573 *irregularis*. Expression values were normalized against *GAPDH*. Points indicate individual plants.  
574 Means groups were calculated *post hoc* independently for the two transcripts and are indicated by  
575 letters ( $p < 0.05$ ).

576



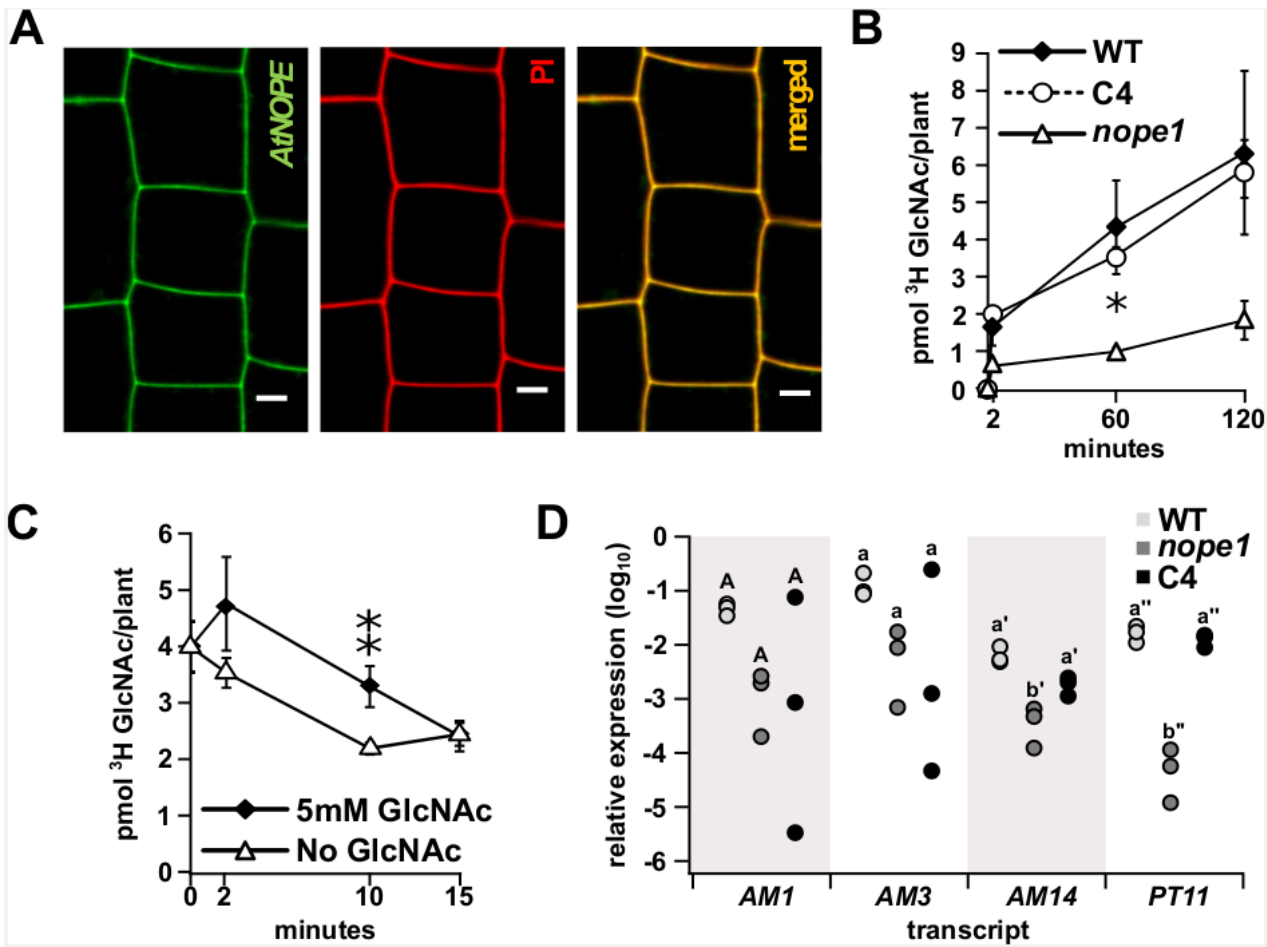
578

579 **Figure 4. Rice NOPE1 mediates GlcNAc transport in *C. albicans*.** A, Ten-fold cell dilution  
 580 series of *C. albicans* strains spotted onto plates with indicated sugar. B, *C. albicans* strains grown  
 581 overnight in glucose containing medium and resuspended in fresh medium containing either 50  
 582 mM glucose or 50 mM GlcNAc. C, [<sup>3</sup>H]GlcNAc uptake in *C. albicans* strains at 20mM and  
 583 200mM GlcNAc. GlcNAc, N-acetylglucosamine. Boxes show 1st quartile, median and 3rd  
 584 quartile. Whiskers extend to the most extreme points within 1.5x box length; outlying values

585 beyond this range are shown as unfilled circles. Means groups were calculated *post hoc*  
586 indepently for the two GlcNAc treatments and are indicated by letters (  $p < 0.05$ ). For description  
587 of strains see Supplemental Information Table 5.

588

589

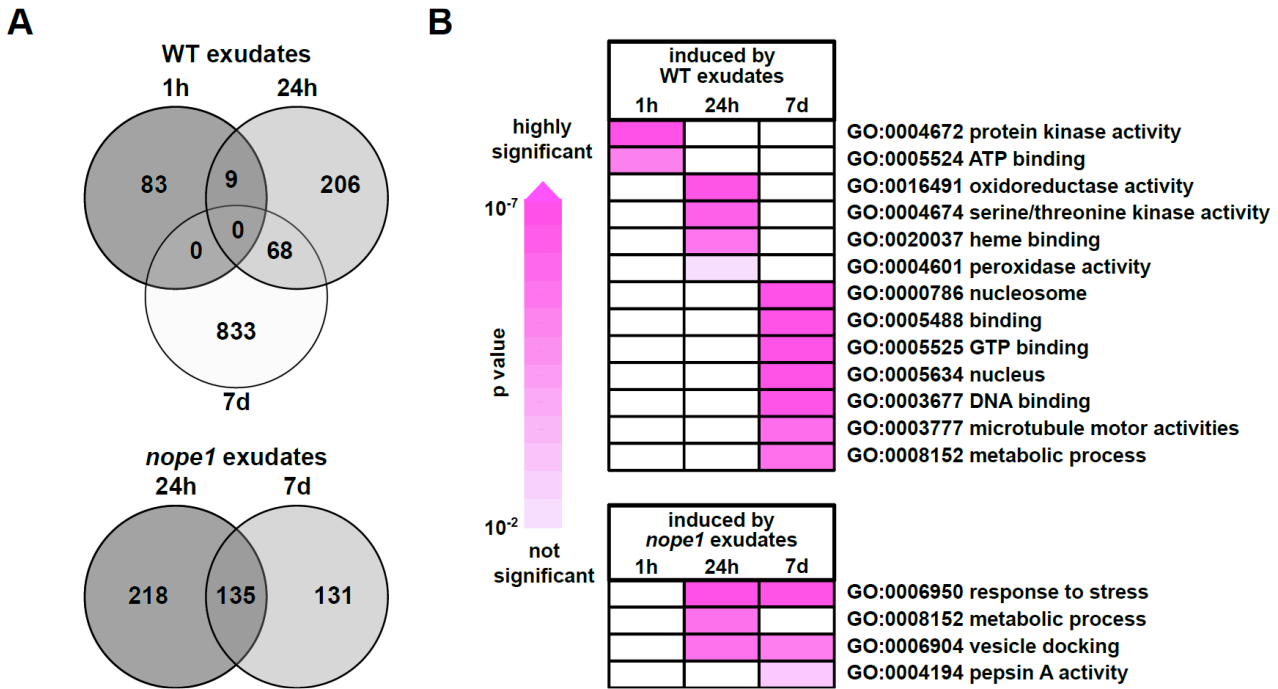


591

592 **Figure 5. NOPE1 mediates GlcNAc transport in rice and Arabidopsis.** **A**, Laser scanning  
 593 confocal microscopy of *A. thaliana* roots expressing  $Ubq_{prom}::YFP::AtNOPE1$  (line *At4731y-4*).  
 594 YFP-AtNOPE1 signal shown in green (left). Corresponding cells stained with Propidium Iodide  
 595 (PI) shown in red (centre). Overlay (yellow, right). Scale bar: 5 $\mu$ m. **B**, Time course of  
 596 [ $^3H$ ]GlcNAc uptake in roots of *Osnope1*, wild type and genetically complemented mutant line C4.  
 597 Means and SEs of three biologically independent experiments are shown (\* $P \leq 0.05$ ) **C**, Time  
 598 course of [ $^3H$ ]GlcNAc export activity of wild type rice roots at 0 and 5mM (50X) GlcNAc  
 599 external concentration. Means and SEs of three biological replicates are shown. (\*\* $p \leq 0.01$ ). **D**,  
 600 qRT-PCR-based analysis of *AM1*, *AM3*, *AM14*, and *PT11* marker transcript accumulation in the  
 601 roots of wild type, *Osnope1*, and the complemented line C4, at 6 wpi with *R. irregularis*.  
 602 Expression values were normalized against *CYCLOPHILLIN* (*LOC\_Os02g02890*). Points  
 603 represent individual plants. Means groups were calculated *post hoc* independently for each transcript  
 604 and are indicated by letters ( $p < 0.05$ ).

605

606



608

609

610

611 **Figure 6. *R. irregularis* transcriptional response to root exudates from rice wild type and**  
 612 ***Osnope1* mutant plants. A,** Venn diagrams indicating number of significantly induced fungal  
 613 genes ( $P \leq 0.05$ , one way ANOVA) in response to treatment with exudates from wild type relative  
 614 to *Osnope1* (top) and *Osnope1* relative to wild type (bottom). **B,** Time-resolved Gene Ontology  
 615 analysis for Biological Process terms ( $p \leq 0.01$ ) for fungal genes induced when treated with root  
 616 exudates from wild type (top) or from *Osnope1* (bottom). The colour code indicates the  
 617 significance of gene enrichment (p-value).  
 618